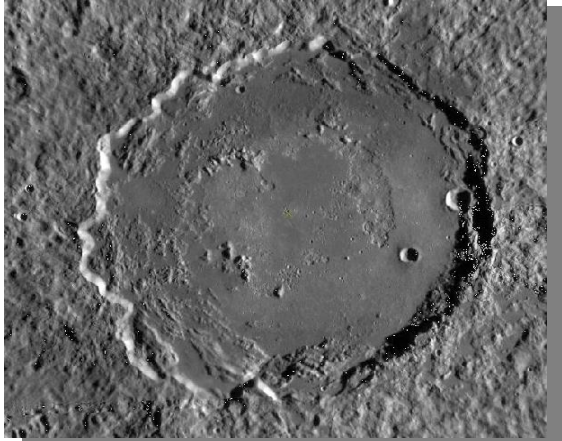


**PERIPHERAL PEAK RINGS ON MERCURY AND IMPLICATIONS FOR NEAR SURFACE GEOLOGY AND ANALYSIS OF CRATER POPULATIONS.** F. Ciceri<sup>1,2</sup> and A. R. Hildebrand<sup>1</sup>, <sup>1</sup> Department of Geoscience, University of Calgary, Calgary, AB T2N 1N4, <sup>2</sup> Università di Milano-Bicocca, Milan, Piazza della scienza U4, Italy (fabio.ciceri.geo@gmail.com)

**Introduction:** Peripheral peak rings (PPR) have been found on Mars, Venus, and Mercury [e.g. 1, 2]. PPR's result from crater wall retreat through block sliding and collapse, producing both monolithic and rubbly morphologies [2]. We have examined available imagery from NASA's Mariner 10 and MESSENGER spacecraft to map the population of PPR craters on Mercury finding both monolithic and rubbly morphologies (See Fig. 1).



**Figure 1:** MESSENGER image of a 176 km-diameter peak ring crater showing several discontinuous mostly monolithic PPR segments (from ~5 o'clock clockwise to 2 o'clock) with some rubbly PPR. (Long. 19E, Lat. 9S, resolution 166.3 meters/pixel)

On Mars, PPRs preferentially occur where an apparent strong surface layer exists, typically a basalt, over a weak layer (regolith/sediment) [1]. On Mercury the strengths and composition of surface layers is less clear due to the relative low-resolution of imagery and topographic data of MESSENGER and Mariner 10 missions, so that PPR presence, particularly of monolithic PPR, is perhaps an indicator of near surface layering characteristics. The occurrence of block sliding is also indicative of the presence of volatiles (to lubricate the slip plane) based upon 1) observed terrestrial examples of block slides, and 2) that PPR are found on Mars, Venus, and Mercury, but are almost entirely absent on the Moon [2]. Mercury is not highly depleted in volatile elements relative to the other terrestrial planets, as evidenced through fast neutrons and X-ray analysis, and landform development [e.g. 3, 4, 5, 6] allowing a possible role of volatiles in Mercury's PPRs/block sliding. In this study we present 1) the spatial distribution of the PPRs on Mercury, 2) examine correlations between PPR occurrence and other indicators of volatile distribution, and 3) the cumulative size-frequency distribution plot and the R-plot of Caloris Basin showing

some implications of PPR formation on cumulative crater size distributions.

**Methodology:** The study area extends from -65 to 65 in latitude and -180 to 180 in longitude; we used the Mercury MESSENGER MDIS Basemap Global Mosaic [8] with a maximum resolution of ~166 m/pixel. All data were imported into the ESRI ArcMap GIS using a simple cylindrical map projection. The CraterTools [9] extension was used to count craters in the internal part of Caloris Basin (between 141 and -175 in longitude and between 50 and 12 in latitude); this program defines a best fit circle to the crater rim from three points selected along the rim [10]. According to Fasset et al. (2011) [10] craters with diameters < 20 km were excluded due to: (1) the relative low-resolution of MDIS images and (2) to insure that the observed population consists principally of primary impact craters [10].

**PPRs – spatial-distribution:** The spatial distribution of Mercury's PPRs (Fig. 2) reveals that the PPRs are not distributed randomly on the surface (although comparably-sized impact craters are randomly distributed) suggesting significant dependence with the composition or geology of the surface. Plotting the data on spatial distribution of PPRs with two other volatile-related surface features, Single fluidized Layer Ejecta (SLE) craters (red dots, Fig. 2), and the Central Pit craters (yellow triangles, Fig. 2), reveals a similar spatial distribution indicating an apparent stronger dependence on volatile occurrence in the near surface rather than on geological variation of Mercury's surface layers.

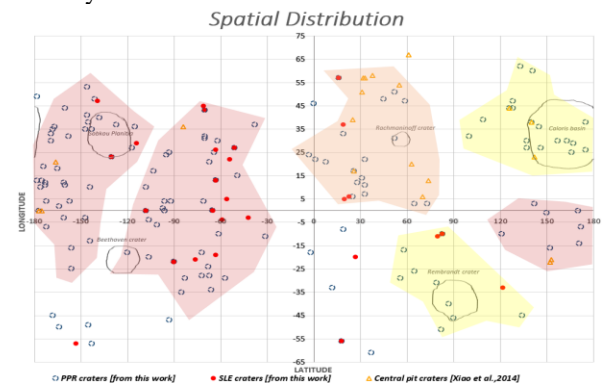


**Figure 2:** Spatial distribution map of PPR (blue circles), SLE craters (red dots) and Central Pit craters (yellow triangles). The areas indicate where PPRs are densely distributed (yellow = low density, orange = medium density, red = high density). The location data of central pit craters are from Xiao et al. (2014) [6]; SLE craters were mapped as part of this work.

The correlation also further implies a key role of volatiles in the formation of PPR. Therefore, PPR can potentially be used as a tracer for the near surface volatile content on rocky planetary surfaces.

**PPR Enlargement of Craters:** Development of PPR in complex craters results in significant retreat of their topographic rims beyond the limits of the zone of slump block formation, resulting in larger apparent diameters (and lower rim heights) which aren't reflective of the cratering process. This in turn can skew analysis of relative and absolute surface ages (and reconstruction of impactor populations) unless pre-PPR crater rims and diameters are reconstructed.

*Caloris Basin.* Cratering data for the internal part of Caloris Basin, are plotted into a cumulative size frequency distribution plot from unbinned data (see [7]). In Fig. 3 crater diameters were plotted without considering where PPR are present. In Fig. 4 crater diameters

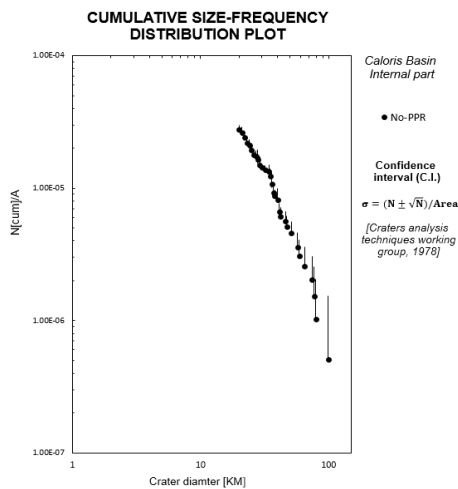


Figure 3: crater cumulative size-frequency distribution plot of the internal part of Caloris Basin.

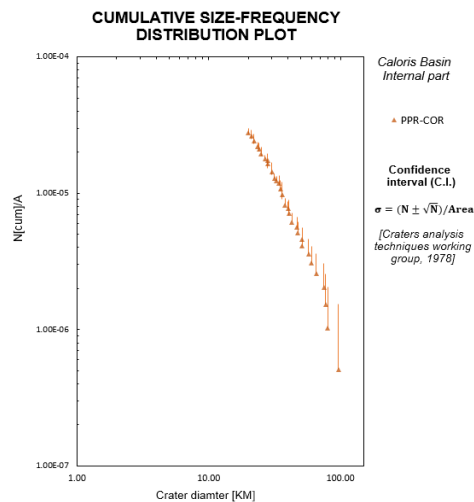


Figure 4: crater cumulative size-frequency distribution of the internal part of Caloris Basin with PPR correction.

were corrected where PPR were present. Using CraterTools a best fit circle was tied to a crater's rim using three points along the rim where PPR formation had not enlarged it.

Comparing the cumulative size-frequency distribution plots in Figs. 3 & 4 shows one significant change; the cumulative curve in Fig. 3 shows a “bump” at crater diameters of ~40 – 50 km diameter. However this “bump” in the cumulative curve disappears (Fig. 4) when the PPR created enlargement is removed. Fig. 5 shows the cumulative curve expressed as an R-plot and again the feature at 40 to 50 km diameter almost disappears once the PPR enlargement is corrected.

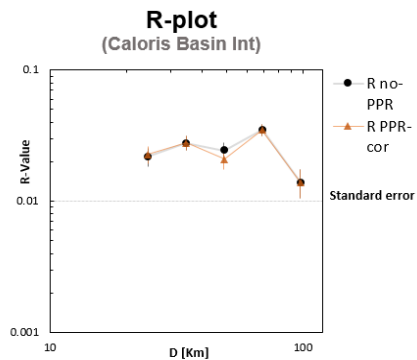


Figure 5: R-Plot of Caloris Basin (Internal part) obtained from binned data using a factor  $2^{1/2}$  (see [7]). The black dots represent the data without PPR-correction. The orange triangles represent the data with PPR-correction.

The preponderance of PPR development in craters around 40-50 km diameter suggests, a possible dependence with crater diameter. This may have some significant implications in the studies of the size-frequency distribution of the craters on Mercury, but this remains to be tested for all regions. For example, to date a surface the observed crater size-frequency distribution is fitted to a known crater production function that describes how many craters of a given size are formed in relation to the number of any other size [11].

**References:** [1] Nycz J. and Hildebrand R. A. (2007) *JGR*, 90, 1151–1154. [2] Nycz J. et al. submitted manuscript. [3] Lawrence D. J. et al. (2017) *Icarus* 281, 32-45. [4] Nittler L. R. (2011) *Science*, VOL 333, 1847-1850. [5] Blewett D. T. et al. (2011) *Science* VOL 333, 1856-1859 [6] Xiao Z. and Komatsu G. (2014) *Planetary and Space Science* 95, 103-119. [7] Crater Analysis Techniques Working Group (1979) *Icarus* 37, 467-474. [8] Johns Hopkins Applied Physics Laboratory MESSENGER Team website. [9] Kneissl T. et al. (2011) *Planetary and Space Science* 59, 1243-1254. [10] Fassett C. I. et al. (2011) *Geophysical Research Letters*, VOL. 38, L10202. [11] Michael G.G. and Neukum G. (2010) *Earth and Planetary Science Letters* 294, 223-229.